La Science à l'œuvre pour le
at work for Canada

NRC Publications Archive
Archives des publications du CNRC

Increases in the proton conductivity and selectivity of proton exchange membranes for direct methanol fuel cells by formation of nanocomposites having proton conducting channels

Su, Yu-Huei; Liu, Ying-Ling; Wang, Da-Ming; Lai, Juin-Yih; Guiver, Michael; Liu, Baijun

National Research
Council Canada

Conseil national
de recherches Canada

Canada

Increases in the proton conductivity and selectivity of proton exchange membranes for direct methanol fuel cells by formation of nanocomposites having proton conducting channels

Yu-Huei Su[a], Ying-Ling Liu[b,*], Da-Ming Wang[a], Juin-Yih Lai[b], Michael D. Guiver[c], Baijun Liu[d]

[a] Institute of Polymer Science and Engineering, National Taiwan University, Taipei 104, Taiwan
[b] R&D Center for Membrane Technology and Department of Chemical Engineering, Chung Yuan University, Chungli, Taoyuan 320, Taiwan
[c] Institute for Chemical Process and Environmental Technology, National Research Council, Ottawa, Ont., Canada K1A 0R6
[d] Alan G. MacDiarmid Institute, Jilin University, Changchun 130012, PR China

ARTICLE INFO

ABSTRACT

We explore an approach to effectively enhance the properties of cost-effective hydrocarbon proton-exchange membranes for application in the direct methanol fuel cell (DMFC). This approach utilizes sulfonated silica nanoparticles (SA-SNP) as additives to modify sulfonated poly(arylene ether ether ketone ketone) (SPAEEKK). The interaction between the sulfonic acid groups of SA-SNP and those of SPAEEKK combined with hydrophilic–hydrophobic phase separation induce the formation of proton conducting channels, as evidenced by TEM images, which contribute to increases in the proton conductivity of the SPAEEKK/SA-SNP nanocomposite membrane. The presence of SA-SNP nanoparticles also reduces methanol crossover in the membrane. Therefore, the SPAEEKK/SA-SNP nanocomposite membrane shows a high selectivity, which is 2.79-fold the selectivity of Nafion® 117. The improved selectivity of the SPAEEKK/SNP nanocomposite membrane demonstrates potential of this approach in providing hydrocarbon-based PEMs as alternatives to Nafion in direct methanol fuel cells.

© 2009 Elsevier B.V. All rights reserved.

1. Introduction

Proton exchange membranes are a key component in the development of direct methanol fuel cells (DMFCs), which are devices for directly transforming chemical energy into electrical energy without producing waste products and environmental problems [1]. The minimum required properties of PEMs used in DMFCs are that they have high proton conductivities, sufficient chemical stability, adequate mechanical strength, and low methanol permeability. Sulfonated perfluoro-polymers like Nafion®, although having high proton conductivity, have the disadvantage of high cost and high methanol crossover [2]. Consequently, there is a considerable amount of research on seeking alternatives for Nafion® [3–5]. Modifications on present PEM materials aimed at property enhancements is also an effective approach to obtain suitable PEMs for DMFC [6–13]. Increases in the PEM sulfonic acid group concentrations generally lead to significant increases in proton conductivities, provided excessive swelling is avoided. Sacrifices in the mechanical properties and an increase in methanol permeability usually accompany high sulfonic acid concentra-

tions [14]. Stabilization or mitigation of methanol permeability can be achieved through polymer blending [15], cross-linking [16] and formation of nanocomposites [17–20]. However, most of the reported approaches adversely affect the proton conductivities. Selectivity, which is defined as the ratio of proton conductivity over the methanol crossover, is a convenient measure for preliminary evaluation of PEM performance for potential DMFC application [21], since high proton conductivity and low methanol crossover are not commonly achieved through a single approach.

The concept of using inorganic reinforcements possessing sulfonic acid groups has been explored to compensate for the decreases in the sulfonic acid concentrations when normally non-sulfonated inorganic materials are used to form nanocomposite PEMs [22–24]. Nagarale et al. [22] prepared poly(vinyl alcohol) hybrid membranes using tetraethyl orthosilicate (TEOS) and mercaptopropylmethyldimethoxysilane (MPDMS) as precursors via sol–gel reactions. Sulfonic acid groups were incorporated onto the resulting inorganic material after oxidation of the –SH groups of MPDMS. Kim et al. reported similar work on PVA/poly(acrylic acid) based PEMs [23]. Rhee et al. [24] utilized sulfonated montmorillonite to modify Nafion® to effectively lower the methanol crossover without decreasing PEM proton conductivities. Chang et al. [25] incorporated sulfonated polyhedral oligosilsesquioxane

---

* Corresponding author. Tel.: +886 3 2654130; fax: +886 3 2654199.
E-mail address: ylliu@cycu.edu.tw (Y.-L. Liu).

(sPOSS) in poly(vinyl alcohol) (PVA) to increase proton conductivities and decrease methanol permeability.

High proton conductivities may also be obtained with PEMs possessing relatively low sulfonic acid contents, if the sulfonic acid groups are able to effectively form proton conducting channels. Approaches to achieve such control of chemical morphology through micro-phase separation are PEM materials derived from polymer blends [15,16], block copolymers [26] and graft copolymers [27]. One example reported by Jung et al. [15] is a polymer blend of sulfonated polystyrene (sPS) and sulfonated poly (2,6-dimethyl-1,4-phenylene oxide) (sPPO). The polymer blend exhibited higher proton conductivities compared to the individual sPS and sPPO membranes due to the formation of proton conducting channels through micro-phase separation. Yang et al. [26] found that although sulfonated polysulfone-b-poly(vinylidene fluoride) block copolymers (sPSF-b-PVDF) possessed relatively low sulfonic acid contents and low ion exchange capacities (IEC), the hydrophobic PVDF chains of the sPSF-b-PVDF block copolymer promote phase separation and induce the acid group aggregation into proton conducting paths. Similar effects and results were also observed with graft copolymers possessing poly(sodium styrenesulfonate) side chains and polystyrene backbones [27]. These studies demonstrated that formation of proton conducting channels is an effective approach to increase the proton conductivities of PEMs without the necessity for high sulfonic acid content. However, the preparation of well-defined block and graft copolymers often requires special molecular design and complex synthetic routes. On the other hand, compared to unfilled PEMs, nanocomposites usually exhibit improvements in mechanical stability and a reduction on methanol crossover. Formation of proton conducting channels in nanocomposite PEMs is therefore an attractive approach to enhance the proton conductivities. Chen et al. [28] reported poly(oxyalkylene)diamine-functionalized carbon nanotube (CNT)/Nafion[®] nanocomposites and postulated that the amino groups of the modified CNTs would promote Nafion[®] coalescing on CNTs through the $-NH_2/-SO_3H$ ionic interactions and thereby provide continuous pathways for proton transport. Kannan et al. [29] also prepared sulfonic acid functionalized single-walled carbon nanotubes (s-SWNT)/Nafion[®] nanocomposite membranes. The presence of s-SWNT was postulated to promote the formation of channel-like networks of sulfonic acid groups for proton transport. However, the formation of proton conducting channels in the nanocomposite PEMs is still only a postulation. Our previous papers also reported that silica nanoparticles are effective as additives for PEMs for enhancing the properties of PEMs for use in DMFC [30,31].

The fluorinated moieties in sulfonated poly(arylene ether ether ketone ketone) (SPAEEKK) increase the hydrophobicity of polymer and enhance the formation of separated hydrophobic and hydrophilic domains in its microstructure, thereby providing the proton conducting domains [32]. Addition of silica to SPAEEKK membranes through the sol–gel process formed hybrid membranes, which showed decreased methanol crossover. Acid-doping the SPAEEKK/silica hybrid membranes with H_3PO_4 increased their proton conductivities [33]. In the present work, SPAEEKK is modified with sulfonated silica nanoparticles (SA-SNP) which provides the above-mentioned combined effects of silica nanoparticles and acid groups. The fluorine-containing moieties of SPAEEKK impart hydrophobicity and promote micro-phase separation between the hydrophilic sulfonic acid and the hydrophobic portions in the SPAEEKK/SA-SNP nanocomposite membranes. The interaction between the $-SO_3H$ groups of SA-SNP and SPAEEKK induces the acid groups to aggregate into ionic domains. Both of the above-mentioned mechanisms facilitate the formation of sulfonic acid groups into continuous proton transport domains, i.e. the proton conducting channels, which was observed by transmission electron microscopy (TEM). Moreover, the methanol permeabil-

ity of SPAEEKK was significantly reduced by the formation of nanocomposites with SA-SNP. The combined effect of increasing proton conductivity and decreasing methanol permeability improves selectivity [21,34] of SPAEEKK/SA-SNP membranes.

2. Materials and methods

2.1. Materials

Sulfonated poly(arylene ether ether ketone ketone) (SPAEEKK) copolymer containing pendant naphthalene sulfonic acid groups was synthesized from the commercially available monomers sodium 6,7-dihydroxy-2-naphthalene sulfonate (DHNS), 1,4-bis(4-fluorobenzoyl)-benzene (BFBB), and hexafluorobisphenol A (6F-BPA) [33]. The sulfonic acid content (SC, the number of sulfonic acid groups per repeating unit of PAEEKK) of the utilized SPAEEKK was 0.67. Silica nanoparticles (SNP) with a size of 10–20 nm were purchased from Nissan Chemical Company. Sulfonated silica nanoparticles (SA-SNP) were obtained by sulfonation of SNP according to the reported method [35,36]. The sulfur content of SA-SNP was 1.82 wt% by elemental analysis, which corresponds to a sulfonic acid equivalent concentration of 0.5687 mol g^{-1} for SA-SNP. N,N-dimethylacetamide (DMAc) and methanol (MeOH) were reagent grade. Distilled water was used in all experiments.

2.2. Preparation of SPAEEKK nanocomposite membranes

SPAEEKK (1.0 g, Fig. 1) was dissolved in 12 mL of DMAc and the solution was filtered using a filter having 1 μm pore size. A measured amount of SA-SNP (50 mg of SA-SNP/g of SPAEEKK) was added into the solution and stirred for 1 day, which resulted in a homogeneous solution-suspension. This solution-suspension was poured onto a glass plate and dried at 40 °C for 2 days. The residual solvent was evaporated at 80 °C for another 2 days. The membrane was removed from the glass plate by soaking it in water. The membranes were soaked in 1N H_2SO_4 for more than 48 h at room temperature followed by immersion in several wash baths of distilled water for more than 12 h at room temperature to remove excess acid. The tough flexible, yellowish transparent membranes (SPAEEKK/SA-SNP) were obtained after air-drying at ambient temperature. The other membrane (SPAEEKK/SNP) made of SPAEEK and SNP (non-sulfonated) was prepared in the same manner.

The nomenclature used for the membranes described in this article is as follows. SP/SNP and SP/SA-SNP relate to SPAEEKK/silica nanoparticle and SPAEEKK/sulfonated silica nanoparticle nanocomposite membranes, respectively.

2.3. Measurements and property evaluation

2.3.1. Instrumental analysis

Thermogravimetric analysis was conducted with a Perkin Elmer TGA-7. Polymer samples for TGA measurements were preheated to 150 °C under a nitrogen atmosphere, held isothermally for 60 min, equilibrated at 80 °C, and then heated to 800 °C at a heating rate 10 °C/min. The fractions of free water in membranes were determined by differential scanning calorimeter (Perkin Elmer DSC 7), using a heating rate of 5 °C/min and with a nitrogen flow rate of 100 mL/min.

2.3.2. Ion exchange capacity (IEC) and fixed ion concentration

IEC values were measured using the classical titration technique. After immersing the membrane samples in distilled water, they were soaked in a large volume of 0.1 M HCl solution to ensure conversion of sulfonic groups into the H$^+$ form. The samples were then washed thoroughly with distilled water to remove excess HCl, and then were immersed in 1 M NaCl solution to convert sulfonic acid
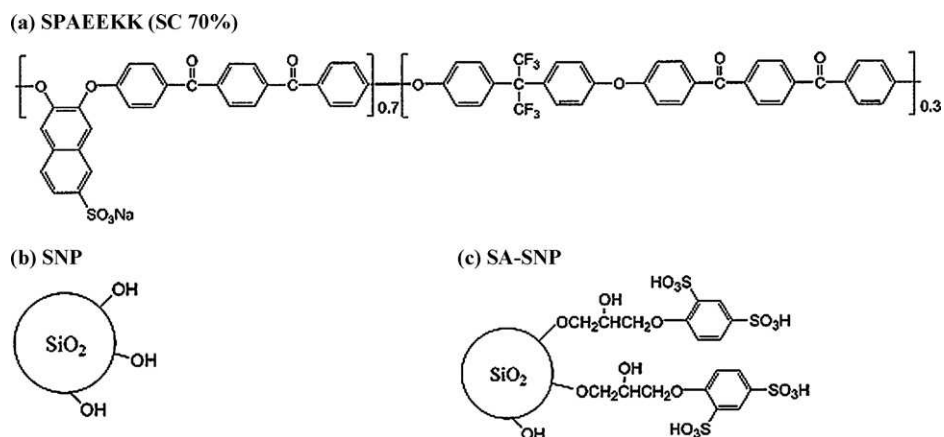
Fig. 1. Chemical structures of (a) polymer electrolyte SPAEEKK (SC 70%) [33];(b) SNP and (b) SA-SNP [35,36] used in this work.

to sodium form. The released H$^+$ was back titrated with a 0.01 M NaOH solution using phenolphthalein as indicator. The volume of NaOH and pH was recorded to determine the equivalence point. The IEC value (in meq/g) is defined as milliequivalents of sulfonic groups per gram of dried sample and it is obtained from the following equation: IEC = $(M_{O,NaOH} - M_{E,NaOH}/W_{dry})$ where $M_{O,NaOH}$ is the milliequivalent (meq.) of NaOH in the flask at the beginning of the titration, $M_{E,NaOH}$ is the meq. of NaOH after equilibrium, and W_{dry} is the weight of the dry membrane (g). The fixed ion concentration (in meq/g of H$_2$O) was calculated as the ratio of the IEC value to the water content.

2.3.3. Water and methanol uptake

The membrane samples were vacuum dried at 120 °C before testing. The sample films were soaked in de-ionized water until swelling equilibrium was attained at predetermined temperatures. The dry weight and the equilibrated swollen weight of the membranes were determined. Swollen membranes were blotted dry with tissue paper before weight measurements. The apparent water or methanol uptakes of the membranes were determined as follows: Uptake content (%) = $(W_s - W_d/W_d) \times 100\%$ where W_s and W_d are the weights of swollen and dried samples, respectively.

2.3.4. Methanol permeation measurement by pervaporation process

The experiment was carried out according to a reported procedure [37]. The feed solution was in direct contact with membrane, in the pervaporation apparatus. The effective membrane area was 6.7 cm^2 and the experiments were conducted with a 50 °C feed solution. The permeation rate was determined by measuring the weight of permeate. The compositions of feed solution and permeate were analyzed by a gas chromatography (GC China Chromatography 8700T). The separation factor of water/alcohol ($\alpha_{W/A}$) was calculated from:

$$\alpha_{W/A} = \left(\frac{Y_W/Y_A}{X_W/X_A} \right)$$

where X_W, X_A, Y_W, Y_A are the weight fraction of water and alcohol in the feed and permeate, respectively.

2.3.5. Proton conductivity

The proton conductivity was measured by alternating-current (ac) impedance spectroscopy over a frequency range of 1–10^7 Hz with an oscillating voltage of 50–500 mV with a system based on a Solartron 1280 gain phase analyzer. A sample with a diameter of 3.5 mm was placed in an open, temperature-controlled cell, in which it was clamped between two blocking stainless steel elec-

trodes with a permanent pressure of about 3 kg cm^{-2}. Specimens were soaked in de-ionized water before the test. The conductivity (σ) of the samples in the transverse direction was calculated from the impedance data, with the relationship $\sigma = d/RS$, where d and S are the thickness and face area of the sample, respectively, and R was derived from the low intersection of the high frequency semicircle on a complex impedance plane with the $Re(Z)$ axis.

3. Results and discussion

3.1. Preparation of SPAEEKK membranes and nanocomposite membranes

The chemical structures of SPAEEKK, SNP, SA-SNP are shown in Fig. 1. Homogeneous SP/SA-SNP and SP/SNP membranes were obtained by casting using DMAc as a solvent. The membranes show high transparency, suggesting that the silica nanoparticles do not aggregate in the membranes during membrane preparation. The compatibility between SPAEEKK and SA-SNP is highly enhanced by formation of ionic aggregates between SPAEEKK and SA-SNP [26], which act to cross-link the SP/SA-SNP nanocomposite membranes. The formation of cross-linked structure in the SP/SA-SNP membrane was demonstrated by its insolubility in DMAc, since the pristine SPAEEKK membrane is readily soluble in the same solvent. Cross-linking in the SP/SA-SNP nanocomposite membrane should enhance the membrane stability in solvents and reduce the methanol permeability, which are positive attributes for application as proton exchange membranes for DMFC. On the other hand, the absence of sulfonic acid groups in SNP does not enable the same type of ionic cross-linking to occur in the SP/SNP membrane, as demonstrated by its good solubility in DMAc. However, the hydrogen-bonding between SPAEEKK and SNP still provides some interaction between these two materials so as to enhance their compatibility and to promote the dispersion of SNP particles within the SPAEEKK matrix.

The thermal stability of the SPAEEKK-based membranes was measured with a thermogravimetric analyzer (TGA). The thermograms of the membranes are shown in Fig. 2. All three samples exhibited similar TGA curves showing a two-stage weight loss at about 300 and 550 °C. The first stage weight loss is associated with the loss of the sulfonic acid groups and the second one with the decomposition of the SPAEEKK main chains. The interaction between silica nanoparticles and SPAEEKK enhances the thermal stability of the sulfonic acid groups of SPAEEKK, shifting the first stage weight loss to higher temperatures. The temperature shift is more significant for SP/SA-SNP membrane. However, the presence of SNP or SA-SNP nanoparticles does not alter the weight loss
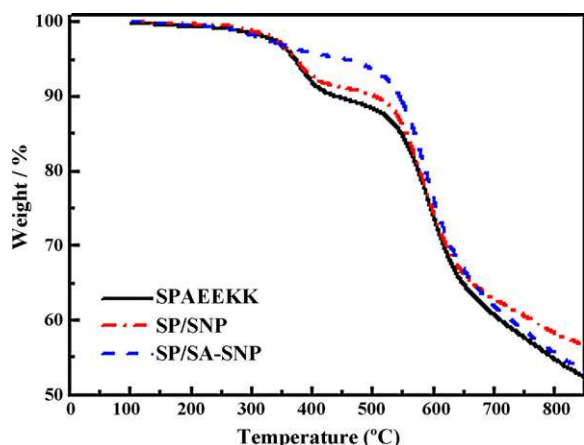
Fig. 2. Thermo-gravimetric analysis (TGA) of SPAEEKK and nanocomposite membranes.

Fig. 3. Water and methanol weight uptake measured on SPAEEKK and nanocomposite membranes.

behavior of the membranes at 500–600 °C, indicating the nanoparticles are not involved in the degradation reactions of the polymer main-chain [36].

3.2. Ion exchange capacity, water uptake and fixed ion concentration in the SPAEEKK membranes

The theoretical and measured ion exchange capacities (IEC) of the membranes are shown in Table 1. The theoretical IEC value of SPAEEKK is about 1.30 mmol g^{-1}, and that of SA-SNP is approximately 0.58 mmol g^{-1} according to the literature [33,35]. The theoretical values of SPAEEKK nanocomposite membranes were calculated based on composition. Formation of nanocomposite membranes with silica nanoparticles would decrease the polymer IEC value. However, the sulfonic acid groups of SA-SNP provide some compensation to the IEC value reduction. Therefore, the IEC value calculated for SP/SA-SNP is a little higher than that for SP/SNP. The measured IEC values for SPAEEKK and SP/SNP are a little lower than their calculated values. The difference between the measured and calculated IEC values is relatively large for SP/SA-SNP. This is attributed to the ionic aggregate structure in SP/SA-SNP [26]. The ion clusters of SA-SNP surrounded with hydrophilic segments of SPAEEKK might hinder the ion exchange in the back-titration method. However, addition of sulfonated additives to SPAEEKK, compared to the non-sulfonated additives, would increase the sulfonic acid concentrations in the composite membranes [24].

Water uptake and dimensional swelling of proton exchange membranes, which correlate to the membrane stability, are usually dependent on the IEC value, proton conductivity, and mechanical strength of the membranes. The amount and state of water absorbed by the membrane have been characterized and shown to influence the ionomer microstructure, cluster and channel size in the membrane and to alter the mechanical properties of the membrane [38]. The water uptake and methanol/water mixture (methanol concentration of 3 M) uptake of the SPAEEKK-based membranes were measured at room temperature and the results

are shown in Fig. 3. Theoretically, incorporation of SNP and SA-SNP might provide additional binding sites to water molecules and increase the water uptakes of the membranes. However, the experimental results show an opposite tendency. Formation of nanocomposites with SNP and SA-SNP depressed the water and methanol uptake. The observed decrease was greater for SA-SNP than for SNP nanocomposites. This may be attributed to a restriction of SPAEEKK chain mobility through formation of hydrogen bonding and ionic cross-linking. Moreover, some water-absorption sulfonic sites of SPAEEKK might be blocked with SA-SNP, so as to further reduce the water/methanol uptakes of the SP/SA-SNP membrane. Fig. 4 shows the fixed ion concentrations (*Aw*), which corresponds to the amount of sulfonic acid group per gram of absorbed water in the wet SPAEEKK-based membranes. The *Aw* value can be used as an indicator for the proton conductivity [39], i.e. the higher the fixed ion concentration is, the higher proton conductivity the membrane has. As the water uptake of SP/SA-SNP membrane is reduced, it is expected to show a higher *Aw* value and higher proton conductivity among the three types of membranes.

3.3. Methanol permeability of SPAEEKK membranes and nanocomposite membranes

Fuel crossover through the proton exchange membrane is one of the key issues in DMFC. A reduction in methanol/water uptake

Table 1
IEC values of SPAEEKK and nanocomposite membranes.

Membrane	Theoretical IEC (meq g^{-1})	Measured IEC (meq g^{-1})
SPAEEKK	1.3	1.28 ± 0.01
SP/SNP[a]	1.24	1.21 ± 0.01
SP/SA-SNP[a]	1.27	1.04 ± 0.02
SA-SNP	0.58	–
Nafion® 117	0.91	0.91 ± 0.01

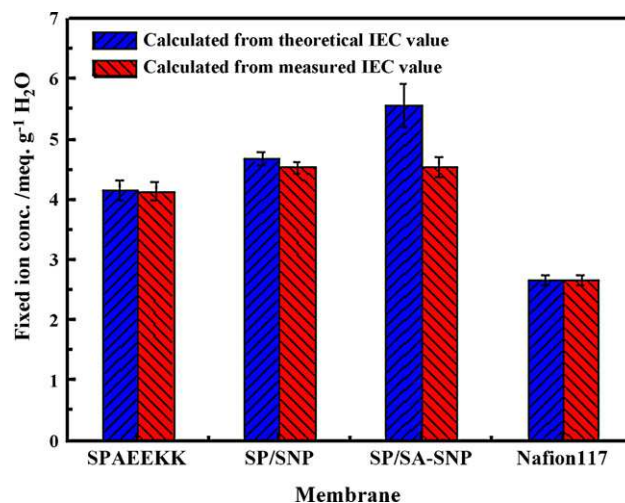[a] The theoretical values were calculated based on composition.

Fig. 4. Fixed ion concentrations of SPAEEKK and nanocomposite membranes.
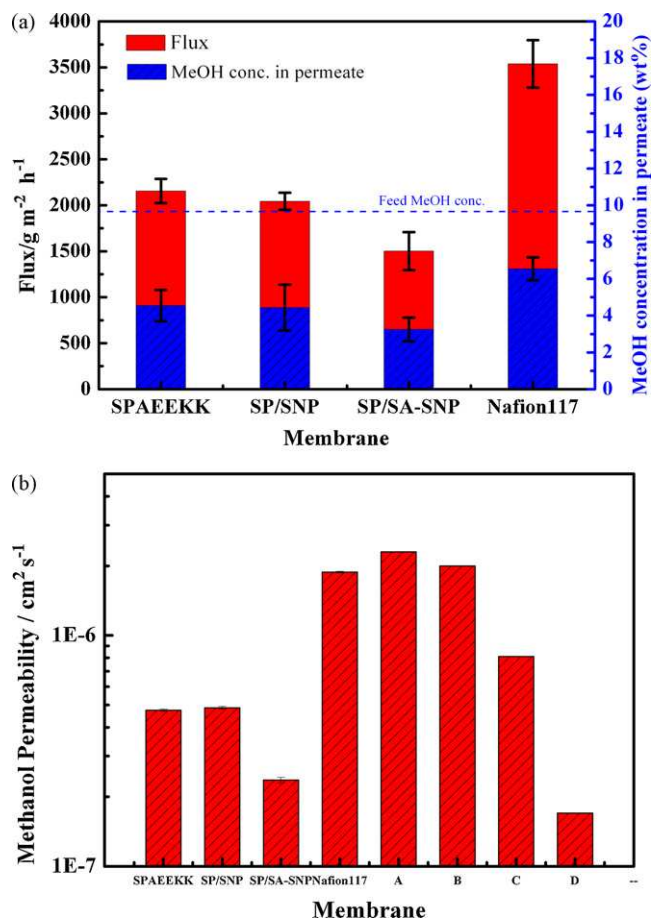
Fig. 5. (a) Methanol and water crossover through SPAEEKK and nanocomposite membranes from a pervaporation method; (b) Methanol permeability of SPAEEKK and nanocomposite membranes. Data of other membranes from literature is included for comparison. Membrane A: sulfonated poly(arylene ether ketone) [42]; Membrane B: Sulfonated poly[styrene-b-(ethylene-r-butylene)-b-styrene] copolymer [43]; Membrane C [12]: Sulfonated poly(arylene ether sulfone) (BPSH) copolymers; Membrane D: sulfonated poly(ether ether ketone ketones) (SPEEK) [44].

observed in SP/SA-SNP nanocomposite membranes indicates its lower methanol affinity and permeability. Permeation measurements provide information on the transport mechanism and the effect of silica nanoparticles in the membrane [40]. Here the methanol permeabilities of nanocomposite membranes were measured by a pervaporation test, and the results are shown in Fig. 5(a). For a 3 M methanol feed solution, the methanol concentrations on the permeate side were lower than the feed side for all membranes. The unfilled membrane exhibited the highest flux and the highest methanol concentration in the permeate. The formation of nanocomposite membranes with SA-SNP significantly decreased the permeation fluxes through the membrane and the methanol concentration in the permeate. The presence of SA-SNP reduced methanol crossover through the membrane by means of both reduction of flux and enhancement of methanol selectivity. The results are coincident to those observed for water uptake data discussed above.

The results of the pervaporation experiments were converted into methanol permeability values by a reported method [41] (Fig. 5 (b)). Silica modification reduces the methanol permeability of SPAEEKK membranes. The methanol permeability of SP/SA-SNP membrane is 4.86×10^{-7} cm^2 s^{-1}, which is much less than that of Nafion®117 (1.87×10^{-6} cm^2 s^{-1}, 3 M methanol aqueous solution in feed, at 70 °C). The methanol permeability of SP/SA-SNP mem-

brane is also lower than or comparable to the values reported to other hydrocarbon PEMs [12,42–44]. Moreover, the effect of SA-SNP on the reduction of the methanol permeability is noteworthy. It is known that methanol permeates through hydrophilic ionic channels. In SP/SA-SNP nanocomposite membrane, the strong ionic interactions between SPAEEKK and SA-SNP suppress the polymer chain mobility and the degree of swelling of the membrane in methanol aqueous solution, so as to reduce the channel size for methanol molecules passing through the membrane. Hence, SA-SNP particles act as blocking materials for methanol transport in the nanocomposite membrane.

3.4. The state of water in the membrane

The proton transport phenomena that occur in sulfonated polymer electrolyte membranes are complex. The Grotthuss mechanism and vehicular diffusion are believed to be the predominant modes of proton conduction [45,46]. In the vehicle mechanism, the proton diffuses together with solvent molecules by forming a complex such as H_3O^+, $CH_3OH_2^+$, and $H_5O_2^+$. In the Grotthuss mechanism, however, the protons jump from one solvent molecule to the next through hydrogen bonds [47]. Hence, water is vital to the proton transport through proton exchange membrane. The presence of additional water enhances proton conductivity via enhancement of proton mobility, as opposed to additional water which lowers conductivity through the dilution effect. In the reported literature [48–51], the water absorbed in the membrane can be divided broadly into two groups of bound water and free water. The bound water is the state of water associated with the membrane matrix whereas the free water is not. These two states of water exhibit different calorimetric behaviors and can be detected with DSC measurements [51,52]. After cooling the membrane to below 0 °C, free water will freeze whereas bound water is nonfreezing. Therefore, for a heating scan on the frozen membrane sample, the heat required to melt the frozen free water can be calculated. The amount of free water in the membrane is obtained by comparing the melting enthalpy of free water to the heat of fusion of pure water (334 J g^{-1}) [49]. The amount of bound water is then obtained from the difference between the total water uptakes and the free water calculated from DSC analysis. The water content, the state of water, and bound water/total water ratio in SPAEEKK membranes are shown in Fig. 6. The amount of all kinds of water in the membranes decreased in the order SPAEEKK > SP/SNP > SP/SA-SNP. Furthermore, the ratio of the bound water to the total water is different for the SPAEEKK-based membranes, indicating that the state of water in the membranes changes with the presence of SNP and SA-SNP nanoparticles. SP/SA-SNP shows the highest bound water/total water ratio among the three examined membranes. The effect of SA-SNP on water content introduces two contradictory aspects: (i) a hygroscopic effect [53] due to the nanocomposite membrane possessing sites that can absorb water, those being both the silica particles and the sulfonic acid groups, which act to increase the content of bound water; (ii) a cross-linking effect due to the inorganic network [23], which reduces polymer chain mobility (free volume) and the space where absorbed water can be accommodated, especially in the case of SA-SNP that gives rise to a more rigid and compact polymer structure. Therefore, with the addition of SA-SNP, the cross-linking effect is more prominent than the hygroscopic effect. This led to the total decrease in water content, whereas the bound water/total water ratio of SPAEEKK nanocomposite membranes increase. The bound water probably participates by the Grotthus mechanism and the free water takes part by a vehicle mechanism and a Grotthus mechanism [33]. The increases in the bound water would increase the contribution of the Grotthus mechanism, especially for the case of free water evaporation at high temperatures. Hence, the SP/SA-SNP nanocomposite mem-
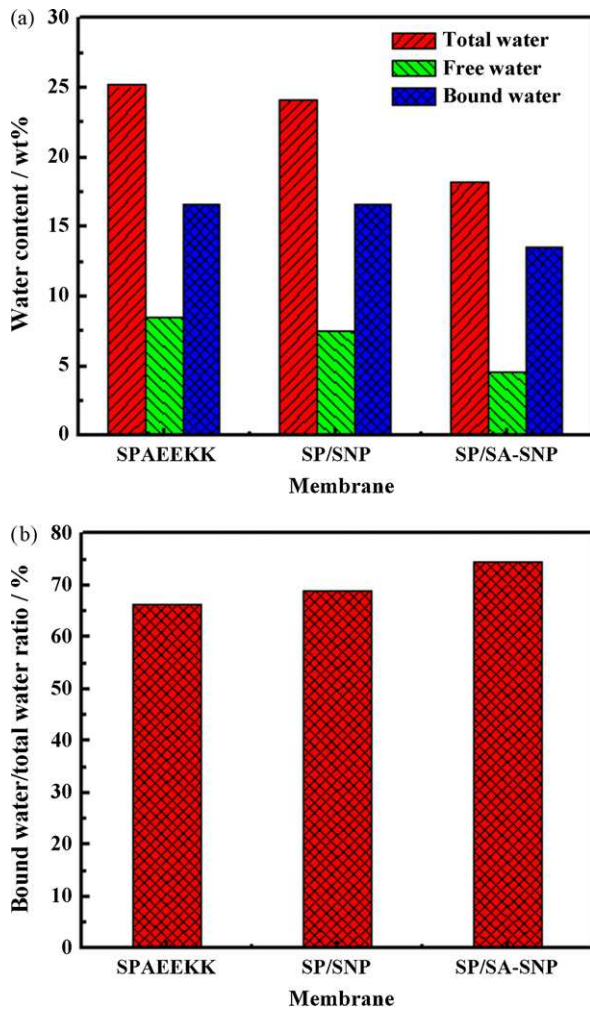
Fig. 6. The water content and the state of water in SPAEEKK and nanocomposite membranes.

Fig. 7. Proton conductivity of the SPAEEKK and nanocomposite membranes at various temperatures.

brane is expected to exhibit a relatively higher proton conductivity and lower methanol permeability among the three types of membranes.

3.5. Proton conductivity of the membranes

The proton conductivity of the proton exchange membrane is a key property affecting operational fuel cell performance. The proton conductivity of the nanocomposite membranes measured at different temperatures is shown in Fig. 7. All of the membranes showed high proton conductivities at high temperatures. Addition of SNP to SPAEEKK caused a reduction in sulfonic acid group concentration so as to lower the proton conductivity of the membrane. This reduction in proton conductivity is somewhat compensated with using SA-SNP as the reinforcement, as SP/SA-SNP membrane exhibits higher proton conductivities than did SPSNP membrane. It is also noteworthy that the proton conductivities of SP/SA-SNP membranes measured at elevated temperatures are higher than the values of the unfilled membrane, even though the measured IEC value of SP/SA-SNP is less than that of the pristine SPAEEKK membrane. It is feasible that a high bound water content in the SP/SA-SNP membrane contributes to the facilitation of proton transport. However, the amount of the total water and the amount of the bound water in SP/SA-SNP nanocomposite membranes are not as high as those in the pristine SPAEEKK membrane. Therefore, SP/SA-SNP could pro-
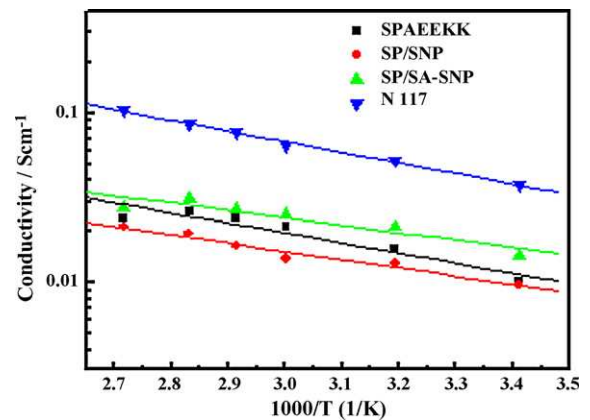
vide another mechanism to promote the proton conducting through the membrane.

The addition of SA-SNP to SPAEEKK could possibly further enhance proton conductivity through restructuring hydrophilic channels in the membrane [50]. The sulfonic acid groups attached to the silica surfaces have restricted motion in the polymer matrix due to the interactions between the sulfonic particle and matrix. These interactions could lead to association of the SA-SNP nanoparticles, which are surrounded by the polymer matrix. The above rationale results in the dispersion morphology of SA-SNP in nanocomposite membranes as observed by STEM (Fig. 8). STEM analysis was performed on 60-nm-thick slices of ultramicrotoned Pb^{2+}-stained SPAEEKK and nanocomposite membranes. The darkly stained spot regions represent the localization of ionic and silica particle domains, which could provide proton transport channels. In the SP/SA-SNP membranes, the ionic channels are visibly connected to yield a continuous ionic network, whereas this network is less developed for SP/SNP. The formation of ionic network in the SP/SA-SNP membrane is especially obvious with using the fluorine-containing SPAEEKK matrix. The presence of fluorine imparts more hydrophobicity in SPAEEKK and promotes micro-phase separation of ionic and nonionic regions and the formation of ionic aggregates and network in the nanocomposite membrane. This observation provides direct evidence for the strong association of sulfonated polymer matrix with sulfonated silica particles, leading to different membrane morphology.

Thus, the addition of SA-SNP to SPAEEKK in a fabricated membrane yields promising results for two reasons: (i) the formation and assembly of proton-conduction pathways due to molecular water absorption, strong interaction between sulfonic acid groups of silica and of polymer and the more hydrophobic segments of SPAEEKK facilitated the formation of continuous ionic phase [27], leading to an increase in proton conductivity; (ii) the addition of sulfonated silica can enhance bound water content in the membrane and suppress the free water content and the crossover of the methanol. To explore the possibility of incorporating SA-SNP into polyelectrolyte for DMFC applications, the relative selectivities (the ratio of proton conductivity over the methanol permeability) of the membranes (normalized with the selectivity of Nafion® 117) are calculated and shown in Fig. 9. The proton conductivities and methanol permeabilities of pristine SPAEEKK and Nafion® 117 were previously reported [33]. Consideration of the differences in measurement instruments and methods utilized in the present work, the data we measured for pristine SPAEEKK and Nafion® 117 was utilized. As shown in Fig. 9, addition of SNP to SPAEEKK reduced the membrane selectivity. On the other hand, addition of SA-SNP significantly increased the membrane selectivity. SP/SA-SNP shows
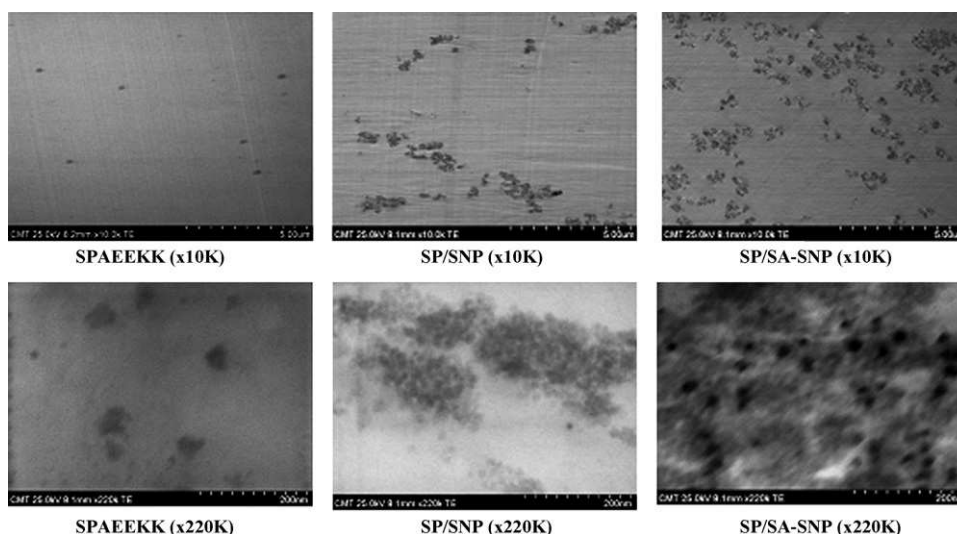
Fig. 8. The FE-STEM images of SPAEEKK and nanocomposite membranes.
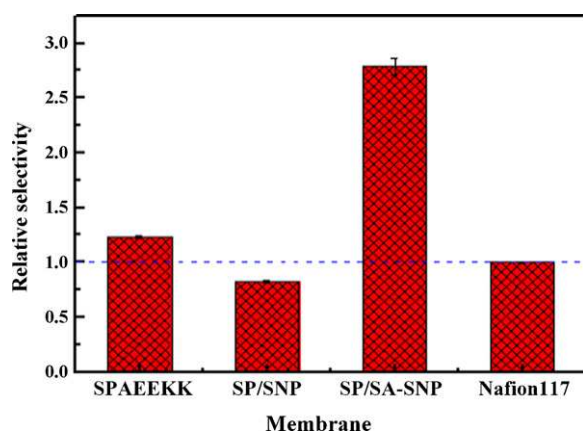

Fig. 9. The relative selectivity of SPAEEKK membranes at 70 °C. (Relative selectivity = selectivity of SPAEEKK membranes/selectivity of Nafion® 117; selectivity = [proton conductivity]/[methanol permeability]).

a high selectivity which is of about 2.79-fold the selectivity of Nafion® 117. Therefore, formation of nanocomposite membranes of sulfonated polyelectrolytes and SA-SNP is an effective approach to improve the polyelectrolyte performances of using in DMFC.

Wholly aromatic PAEEK polymers have relatively good oxidative stability compared to polystyrene derivatives [54]. In this work the
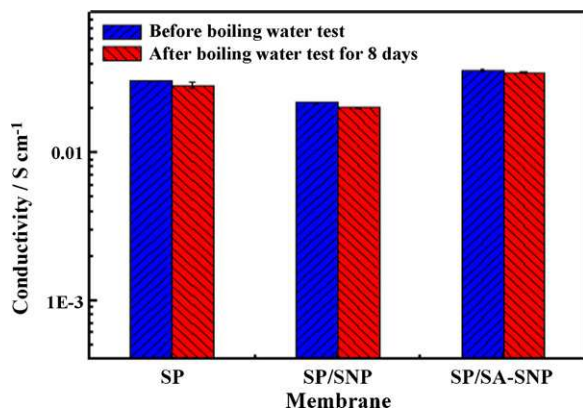

Fig. 10. The hydrolytic stability of SPAEEKK and nanocomposite membranes evaluated by the proton conductivities before and after boiling water test for 8 days.

SPAEEKK based membranes still dissolved into the Fenton reagent in about 1 h because of its high degree of sulfonation [32]. However, the oxidation of hydrocarbon-based membranes in Fenton reagent is not necessarily indicative or a good predictor of their durability under fuel cell operation, since sulfonated poly(ether ether ketone) membranes have shown lifetimes over 1000 h in either PEMFC and DMFC tests [55,56]. Hacker et al. also pointed out that the Fantod's test is not a sufficient gauge for hydrocarbon membranes for DMFCs [51]. On the other hand, the hydrolytic stability of the membranes was examined by immersing the membranes in boiling water for 8 days [50]. Fig. 10 shows the results of the hydrolytic stability test. The membranes do not exhibit significant changes in the proton conductivity after the test, indicating the good hydrolytic stability of the membranes.

4. Conclusions

An effective approach to increase the proton conductivity of low IEC polyelectrolytes is explored through the use of SA-SNP as additives. The −SO_3H groups in the SP/SA-SNP membrane assemble through ionic aggregates between the sulfonic acid groups of SA-SNP and of SPAEEKK to restructure the hydrophilic channels and provide ion conduction pathways in the membrane. The presence of SA-SNP and formation of cross-linked structure in the SP/SA-SNP membrane also decrease the methanol permeability of the membrane, consequently to increase selectivity to be modestly higher than that of Nafion® 117. The higher selectivity of the SP/SA-SNP nanocomposite compared with the other types of SPAEEKK membranes suggests it is a viable approach that can be applied to modify other polymer electrolytes and to enhance the performance of PEMs for DMFC.

Acknowledgements

References

[1] J. Larminie, A. Dicks, Fuel Cell Systems Explained, second ed., John Wiley & Sons Ltd., 2003, 1–24.
[2] T. Norby, Solid State Ionics 97 (1999) 1–9.
[3] C. Genies, R. Mercier, B. Sillion, N. Cornet, G. Gebel, M. Pineri, Polymer 42 (2001) 359–373.

[4] F. Wang, M. Hickner, Y.S. Kim, T.A. Zawodzinski, J.E. McGrath, J. Membr. Sci. 197 (2002) 231–242.
[5] Z.Q. Shi, S. Holdcroft, Macromolecules 37 (2004) 2084–2089.
[6] T. Kobayashi, M. Rikukawa, K. Sanui, N. Ogata, Solid State Ionics 106 (1998) 219–225.
[7] J. Qiao, T. Hamaya, T. Okada, Chem. Mater. 17 (2005) 2413–2421.
[8] S.L. Chen, J.B. Benziger, A.B. Bocarsly, T. Zhang, Ind. Eng. Chem. Res. 44 (2005) 7701–7705.
[9] J. Kerres, C.M. Tang, C. Graf, Ind. Eng. Chem. Res. 43 (2004) 4571–4579.
[10] R.Q. Fu, J.J. Woo, S.J. Seo, J. Power Sources 179 (2008) 458–466.
[11] C.Y. Yen, C.H. Lee, Y.F. Lin, H.L. Lin, Y.H. Hsiao, S.H. Liao, C.Y. Chuang, C.C.M. Ma, J. Power Sources 173 (2007) 36–44.
[12] Y.S. Kim, M.A. Hickner, L. Dong, B.S. Pivovar, J.E. McGrath, J. Membr. Sci. 243 (2004) 317–326.
[13] E. Quartarone, A. Carollo, C. Tomasi, F. Belotti, S. Grandi, P. Mustarelli, A. Magistris, J. Power Sources 168 (2007) 126–134.
[14] M. Sankir, Y.S. Kim, B.S. Pivovar, J.E. McGrath, J. Membr. Sci. 299 (2007) 8–18.
[15] B. Jung, B. Kim, J.M. Yang, J. Membr. Sci. 245 (2004) 61–69.
[16] R. Carter, R. Wycisk, H. Yoo, P.N. Pintauro, Electrochem. Solid-State Lett. 5 (9) (2002) A195–A197.
[17] H.Y. Chang, C.W. Lin, J. Membr. Sci. 218 (2003) 295–306.
[18] B. Ruffmann, H. Silva, B. Schulte, S.P. Nunes, Solid State Ionics 162–163 (2003) 269–275.
[19] P. Costamagna, C. Tang, A.B. Bocarsly, S. Srinivasan, Electrochim. Acta 47 (2002) 1023–1029.
[20] H. Uchida, Y. Ueno, H. Hagihara, M. Watanabe, J. Electrochem. Soc. 150 (2003) A57–A62.
[21] T. Fu, Z. Cui, S. Zhong, Y. Shi, C. Zhao, G. Zhang, K. Shao, H. Na, W. Xing, J. Power Sources 185 (2008) 32–39.
[22] R.K. Nagarale, G.S. Gohil, K. Vinod, R. Shahi, Rangarjan, Macromolecules 37 (2004) 10023–10030.
[23] D.S. Kim, H.B. Park, J.W. Rhim, Y.M. Lee, Solid State Ionics 176 (2005) 117–126.
[24] C.H. Rhee, H.K. Kim, H. Chang, J.S. Lee, Chem. Mater. 17 (2005) 1691–1697.
[25] Y.W. Chang, E. Wang, G. Shin, J.E. Han, P.T. Mather, Polym. Adv. Technol. 18 (2007) 535–543.
[26] Y.S. Yang, Z.Q. Shi, S. Holdcroft, Macromolecules 37 (2004) 1678–1681.
[27] J.F. Ding, C. Chuy, S. Holdcroft, Macromolecules 35 (2002) 1348–1355.
[28] W.F. Chen, J.S. Wu, P.L. Kuo, Chem. Mater. 20 (18) (2008) 5756–5767.
[29] R. Kannan, B.A. Kakade, V.K. Pillai, Angew. Chem. Int. Ed. 47 (2008) 2653–2656.
[30] Y.H. Su, Y.L. Liu, Y.M. Sun, J.Y. Lai, M.D. Guiver, Y. Gao, J. Power Sources 155 (2006) 111–117.
[31] Y.H. Su, Y.L. Liu, Y.M. Sun, J.Y. Lai, D.M. Wang, Y. Gao, B.J. Liu, M.D. Guiver, J. Membr. Sci. 296 (2007) 21–28.
[32] B. Liu, G.P. Robertson, M.D. Guiver, Y.M. Sun, Y.L. Liu, J.Y. Lai, S. Mikhailenko, S. Kaliaguine, J. Polym. Sci.: Part B: Polym. Phys. 44 (2006) 2299–2310.
[33] D.S. Kim, B. Liu, M.D. Guiver, Polymer 47 (2006) 7871–7880.
[34] Y.F. Huang, L.C. Chuang, A.M. Kannan, C.W. Lin, J. Power Sources 186 (2009) 22–28.
[35] Y.L. Liu, C.Y. Hsu, Y.H. Su, J.Y. Lai, Biomacromolecules 6 (2005) 368–373.
[36] Y.L. Liu, C.Y. Hsu, W.L. Wei, R.J. Jeng, Polymer 44 (2003) 5159–5167.
[37] K.R. Lee, Y.H. Wang, M.Y. Teng, D.J. Liaw, J.Y. Lai, Eur. Polym. J. 35 (1999) 861–866.
[38] N. Miyake, J.S. Wainright, R.F. Savinell, J. Electrochem. Soc. 148 (8) (2001) A898–A996.
[39] D.S. Kim, H.B. Park, J.W. Rhim, Y.M. Lee, J. Membr. Sci. 240 (2004) 37–48.
[40] R.C. Jiamg, H.R. Kunz, J.M. Fenton, J. Membr. Sci. 272 (2006) 116–124.
[41] D. Gorri, M.G.D. Angelis, M.G. Baschetti, G.C. Sarti, J. Membr. Sci. 322 (2008) 383–391.
[42] J. Choi, D.H. Kim, H.K. Kim, C. Shin, S.C. Kim, J. Membr. Sci. 310 (2008) 384–392.
[43] H.D. Cho, J. Won, H.Y. Ha, Renewable Energy 33 (2008) 248–253.
[44] X.F. Li, C.P. Liu, H. Lu, C.J. Zhao, Z. Wang, W. Xing, H. Na, J. Membr. Sci. 255 (2005) 149–155.
[45] M. Eikerling, A.A. Kornyshev, A.M. Kuznetsov, J. Ulstrup, S. Walbran, J. Phys. Chem. B105 (2001) 3646–3662.
[46] K.D. Kreuer, Solid State Ionics 94 (1997) 55–62.
[47] K.D. Kreuer, Chem. Mater. 8 (1996) 610–618.
[48] L.E. Karisson, B. Wesslïen, P. Jannasch, Electrochim. Acta 47 (2002) 3269–3275.
[49] S.P. Kusumocahyo, K. Sano, M. Sudoh, M. Kensaka, Sep. Purif. Technol. 18 (2000) 141–150.
[50] J.W. Rhim, H.B. Park, C.S. Lee, J.H. Jun, D.S. Kim, Y.M. Lee, J. Membr. Sci. 238 (2004) 143–151.
[51] B. Gupta, O. Haas, G.G. Scherer, J. Appl. Polym. Sci. 57 (1995) 855–862.
[52] S. Hietala, S. Holmberg, J. Nasman, D. Ostrovskii, M. Paronen, R. Serimaa, F. Sundholm, L. Torell, M. Torkkeli, Angew. Macromol. Chem. 535 (1997) 151–167.
[53] N. Miyake, J.S. Wainright, R.F. Savinell, J. Electrochem. Soc. 148 (2001) A898–A904.
[54] M.A. Hickner, H. Ghassemi, Y.S. Kim, B.R. Einsla, J.E. McGrath, Chem. Rev. 104 (2004) 4587–4612.
[55] J. Rozière, D.J. Jones, Annu. Rev. Mater. Res. 33 (2003) 503–555.
[56] R. Borup, J. Meyers, B. Pivovar, Y.S. Kim, R. Mukundan, N. Garland, D. Myers, M. Wilson, F. Garzon, D. Wood, P. Zelenay, K. More, K. Stroh, T. Zawodzinski, J. Boncella, J.E. McGrath, M. Inaba, K. Miyatake, M. Hori, K. Ota, Z. Ogumi, S. Miyata, A. Nishikata, Z. Siroma, Y. Uchimoto, K. Yasuda, K. Kimijima, N. Iwashita, Chem. Rev. 107 (2007) 3904–3951.